Solar Energy 224 (2021) 1000–1007

Contents lists available at ScienceDirect

Solar Energy

journal homepage: www.elsevier.com/locate/solener

Kinetics of light and elevated temperature-induced degradation in cast mono p-type silicon

Shangzhi Cheng [a,b], Fangxu Ji [a,b], Chunlan Zhou [a,b,*], Junjie Zhu [c], Rune Søndenå [c], Wenjing Wang [a,b], Dongli Hu [d]

[a] The Key Laboratory of Solar Thermal Energy and Photovoltaic System, Institute of Electrical Engineering, Chinese Academy of Science, Beijing, China
[b] University of Chinese Academy of Sciences, Beijing, China
[c] Solar Energy Department, Institute for Energy Technology, Kjeller, Norway
[d] Jiangsu GCL Silicon Material Technology Development Co., Ltd., Jiang su, China

ARTICLE INFO

Keywords:
Cast mono silicon
LeTID
Dark annealing
Illumination
Lifetime

ABSTRACT

Cast mono Silicon (Si) technology has the advantages of low cost, i.e., multicrystalline silicon (mc-Si), and high efficiency, i.e., Czoch-ralski-grown silicon (Cz-Si). Cast mono Si has a similar performance to current Cz-Si counterparts with a solar cell structure, i.e., a passivated emitter and rear cell (PERC). However, the severity of light and elevated temperature-induced degradation (LeTID) on cast mono Si solar cells may be similar to mc-Si, not Cz-Si. To clarify the LeTID kinetics in the p-type cast mono silicon, we observed the effect that LeTID had on the carrier lifetime. First, a series of carrier lifetime measurements were performed to investigate LeTID kinetics in the accelerated regeneration process via high intensity illumination at elevated temperatures and modulating kinetics via dark annealing before illumination. Next, we documented the evolution of a carrier lifetime to investigate the stability of regenerated state at 75 °C and light intensity of ~ 1 kW/m^2. The results show that the effect of dark annealing on LeTID kinetic modulation could be explained by the B-H defect precursor concentration and defect reservoir theory, which originate from the results for mc-Si. An accelerated regeneration method that combines dark annealing and illumination, with high intensity at an elevated temperature, can yield a higher value and improved LeTID stability in terms of the lifetime, as compared with illumination without pre-annealing. This implies that this mixed process may be a potential method to provide both improved performance and high anti-LeTID properties in Si PERC solar cells.

1. Introduction

Since the appearance of light and elevated temperature-induced degradation (LeTID) on p-type mc-Si PERC solar cells in 2012 (Ramspeck et al., 2012), it has been successively observed in p-type Cz-Si, float-zone Si (Chen et al., 2017; Niewelt et al., 2017a), n-type cast-grown mc-Si, and p-type cast mono Si (Sio et al., 2018). LeTID is different the well-known light induced degradation (LID) mechanism, such as B-O complex formation and Fe-B pair dissociation. Continued exposures to the conditions that induce degradation have been shown to lead to an eventual recovery of minority carrier lifetime, often termed 'regeneration.' The underlying mechanisms causing the degradation and regeneration of mc-Si PERC solar cells, however, are still unknown. So far, there are several possible sources of LeTID degradation, including interstitial hydrogen atoms (Ramspeck et al., 2012), transition metal impurities (Eberle et al., 2016). The theories of metal melting dispersion mechanism (Nickel et al., 1996), four-state model introducing of reservoir state of defect precursors (Luka et al., 2016), bucket theory related the transition and movement of hydrogen between different states and positions (Ramspeck et al., 2012) and five-state model for the dark annealing and light soaking effect (Ye et al., 2018) have been put forward respectively.

Cast mono Si is advantageous because it is a low cost, low energy consumption, and large sized technology. Although the dislocation density in cast mono Si can be high compared with Cz-Si (Kaden et al., 2012), previous studies have achieved lifetimes in excess of 1 ms (Stoddard et al., 2016). Moreover, through the optimization of PERC and selective emitter technology, studies have demonstrated that the cast mono Si PERCs can reach an average efficiency of 22.2%, with a maximum efficiency of 22.5%, similar to current Cz-Si counterparts (Lv

* Corresponding author.
E-mail address: zhouchl@mail.iee.ac.cn (C. Zhou).

https://doi.org/10.1016/j.solener.2021.06.054
Received 6 January 2021; Received in revised form 20 June 2021; Accepted 21 June 2021
Available online 1 July 2021

et al., 2020). Although the performance of cast mono Si PERC solar cells can be similar to that of Cz-Si, we aim to investigate whether the degradation and regeneration cycle during LeTID similar to mc-Si because of the existence of defects and impurities (Kutsukake, et al., 2014; Takahashi et al., 2015).

Investigations of LeTID behavior on cast mono p-type Si lifetime samples are still rare and mainly based on solar cells and lifetime samples. Vahlman et al. suggest that light-induced degradation in cast mono Si PERC solar cells involves Cu, introduced during slurry-based wafer slicing (Vahlman et al., 2017). Sio et al. report a lifetime study on the influence of different cooling rates on lifetime degradation and regeneration during the firing process (Sio et al., 2018.). We previously reported the changes of electrical parameters in B-Ga (-P) co-doped cast mono silicon PERC solar cells during light soaking and rapid thermal annealing (Zhou et al., 2020). This study focuses on the degradation and regeneration behavior of LeTID on cast mono p-type Si based on lifetime samples. The advantage of lifetime studies is that they can be useful for the identification of further parameters that influence LeTID behavior because a more flexible experimental design is possible (Zuschlag et al., 2017). In this work, the cast mono silicon samples were illuminated at the following conditions: (i) variable temperature and light intensity during the accelerated regeneration process by illumination and (ii) temperature of 75 °C and light intensity of ~ 1 kW/m^2, which are typical for the examination of the LeTID effect for mc-Si, referred to as the stability test. In addition, a mixed accelerated regeneration method combining dark annealing and illumination, with high intensity at elevated temperature, was applied on both the lifetime samples.

2. Experimental methods

2.1. Silicon lifetime sample preparation

The lifetime samples were prepared on 156.75 mm × 156.75 mm phosphorus compensation B-Ga co-doped cast mono-crystalline Si sourced from GCL Energy Holdings, with a thickness of 180 μm. These neighboring wafers cut from the center of the same ingot were selected to ensure that the electronic properties were as uniform as possible. In the silicon substrate, interstitial O concentrations were 5 ppma, as well as B, Ga, and P concentrations were 1.17 × 10^{16}, 1.42 × 10^{15}, and 5.24 × 10^{15} cm^{-3}, respectively, then the resistivity of approximately was 2 Ω·cm. Saw damage in the wafers was removed in a mixed acid solution of HF and HNO_3. The cast mono P-type Si lifetime samples were then finished in the Cz-Si PERC solar cell production line according to the solar cell production process, including $POCl_3$ diffusion, removing n + -regions, PECVD deposition back-side passivation with a 18 nm AlO_x and 100 nm SiN_x:H, and front-side passivation SiN_x:H films with a thickness of 78 nm and refractive index of 2.1 at 630 nm (MAiA system, Meyer Burger) at a set temperature of 450 °C. Skipping the process of screen printing metal paste, the wafers were directly fired with a temperature profile of the set peak temperature of 880 °C and belt speed of 240 in./min used for industrial PERC solar cells. After firing, the wafers were cut into several pieces of 5 × 5 cm^2 to continue the accelerated regeneration by light soaking at elevated temperature (LS), dark annealing (DA), and LeTID stability test according to the flow-process diagram in Fig. 1.

2.2. Lifetime characterization in the LeTID process

Fig. 1 shows the process sequences and control parameters for DA, LS and LeTID stability test. The accelerated regeneration of the LeTID defects was performed using an LED-based white light soaking system, which has the capability of light soaking at up to an intensity of 7 kW/m^2 and up to 450 °C for the device temperature. Annealing in the darkness was conducted on the hotplate. To test the stability of the treated samples, as-prepared, the regenerated and annealed lifetime samples were placed on a hot plate and then subjected to light soaking at 75 °C under an LED white light source, with an incident irradiance of 1 kW/m^2.

Effective minority carrier lifetimes (τ_{eff}), as a function of excess carrier density Δn, were measured after each process step using a WCT-120 (Sinton Instruments) photoconductance lifetime tester generalized technique (Nagel et al., 1999). Where relevant, lifetimes were extracted at a single Δn of 1 × 10^{15} cm^{-3}. During these experiments, the lifetime samples were taken out for the effective minority carrier lifetime tests at varying time intervals. For example, in the light soaking regeneration experiment, the lifetime measurement was performed every 5 s for the first 5 min and every 60 s thereafter. Before turning on the light source and timing, there was a 20 s waiting time to ensure that the temperature reached the set temperature and stabilized. To compare the maximum sample defect density, the normalized defect density (NDD) was determined based on the lifetime values using Eq. (1) (Niewelt et al., 2017b), where τ(t) is the measured lifetime at time t, τ(t = 0) is the initial lifetime before degradation, and SRH is the Shockley-Read-Hall recombination:

$$= \frac{1}{\tau(t)} - \frac{1}{\tau(t=0)} = 1/\tau_{SRH} \mathrm{NDD} = \frac{1}{\tau(t)} - \frac{1}{\tau(t=0)} = \frac{1}{\tau_{SRH}} \quad (1)$$

The NDD provides a qualitative comparison among the behavior of samples, replacing an absolute assessment of the defect density. Equation (1) eliminates the effect of Auger and band-band recombination, as well as other stabilization defects, such as dislocation. The essential feature is that SRH lifetime, τ_{SRH}, statistics (Eq. (1)) are used to determine the LeTID defect related to SRH recombination with an excess carrier density. The change in the surface passivation during the degradation process was found to be insignificant, such that its impact was also removed by this treatment.

In this study, τ_{SRH} is a linear function of the ratios of total carrier densities (Murphy et al., 2012; Morishige et al., 2016). In p-type material, for example, the SRH lifetime is expressed as a linear function of the ratio of the total electron density (n = n_0 + Δn) to the total hole density

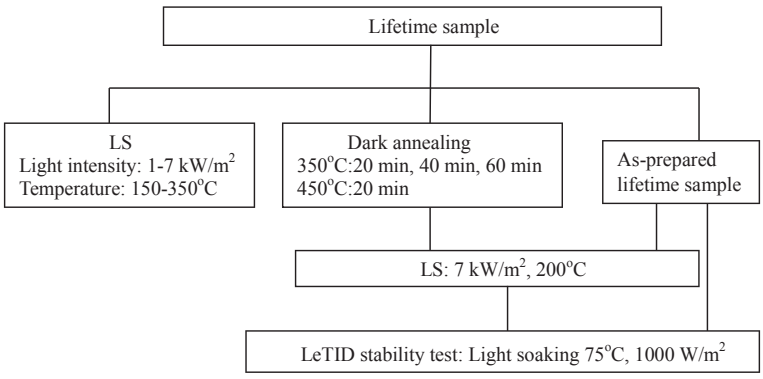

Fig. 1. Process sequences and control parameters for LeTID treatment.

($p = p_0 + \Delta p$) (excess carrier density Δn for electrons and Δp for holes). This ratio is defined as $X = n/p$, because $n_0 \ll \Delta n$ and $n \approx \Delta n = \Delta p$, such that $X = (\Delta n/(\Delta n + p_0))$. Assuming a defect energy level located at the mid-gap of the Si band gap, we can extract the electron and hole capture coefficient ratio Q, and capture cross-section ratio, i.e., $k = \sigma_n/\sigma_p$ calculated by according to $k = \frac{v_{th,e}}{v_{th,h}} Q$ $k = \frac{v_{th,v}}{v_{th,c}} Q$, where $v_{th,e}$ and $v_{th,h}$ is the thermal velocity for electron and hole, respectively in silicon. At 300 K, the $k = Q/1.2$.

3. Results and discussion

3.1. Accelerated regeneration via high intensity soaking at a high temperature

3.1.1. LeTID kinetics during accelerated regeneration

As shown in Fig. 2, the NDD has an evident and strong connection with the substrate temperature and light intensity during high intensity soaking. We can observe the degradation to regeneration cycle of the lifetime for samples treated at the conditions depicted in Fig. 2. The data show that, after light soaking for 2 s, the NDD decreases relative to its initial value due to FeB dissociation to Fe_i during light soaking. The maximum NDD, corresponding to the point of full degradation, decreases with an increase in the temperature (Fig. 2(a)). The effect that light intensity has on the NDD during light soaking is similar to that of the substrate temperature, as shown in Fig. 2(b). The degradation extent decreases with an increasing illumination temperature and light intensity. Moreover, at a higher temperature and light intensity, the degradation rate is significantly more rapid. Higher temperatures and light intensity lead to lower degradation extent, both faster degradation and regeneration rates, which is consistent with the result of mc-Si (Liu et al., 2018a). This connection implies the degradation and regeneration reaction could be accelerated with rising temperature and light intensity.

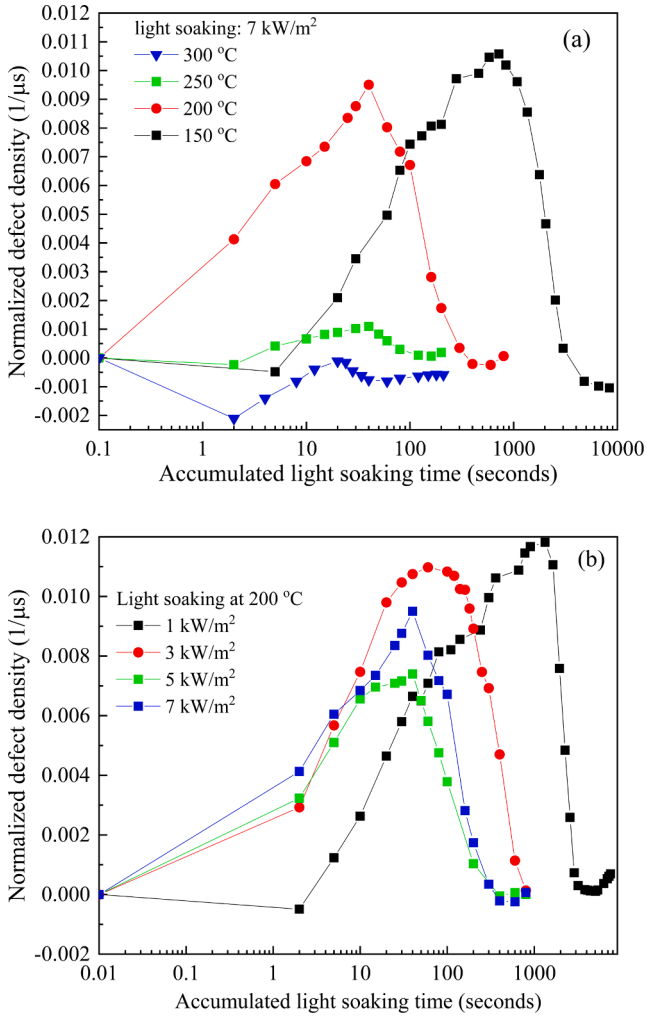

Fig. 2. Normalized defect density with respect to the cumulative time samples exposed to experimental conditions. (a) Data measured at a constant illumination intensity of 7 kW/m^2 at temperatures ranging from 150 to 300 °C. (b) Data for light illumination at 200 °C with variable light intensity.

For all measurements (see Fig. 2), an exponential function, with one growth and one decay phase fit, can be obtained for the full curves to extract the degradation and regeneration time constant according to the formula (Vargas et al., 2019):

$$NDD = NDD_{max}\left[1 - \exp\left(-\frac{t}{\tau_{deg}}\right)\right] - NDD_{max}(1 + A_0)\left[1 - \exp\left(-\frac{t}{\tau_{reg}}\right)\right] \quad (2)$$

Where NDD_{max}, A_0, $\tau_{deg}(\tau_{reg})$ are the maximum value of the NDD, the correction factor and the time constant of degradation (regeneration), respectively.

To determine the defect's active energy, we can obtain an Arrhenius plot of the fitted defect formation and regeneration rate (R = 1/time constant) as a function of inverse temperature (1,000/T) as follows:

$$R = A\exp\left(-\frac{E_a}{K_B T}\right), \quad (3)$$

where, R, A, K_B, T, and E_a correspond to the defect reaction rate, exponential temperature independent pre-factor, Boltzmann's constant, temperature, and reaction activation energy, respectively. Fig. 3 shows the Arrhenius plot of the degradation and regeneration rate constants based on Eq. (3) for the illuminated samples. The Arrhenius activation energies for the defect in the degradation and regeneration stages are 0.48 ± 0.02 eV and 0.70 ± 0.02 eV, respectively. These values are similar to reported values of 0.62–0.78 and 0.67–0.78 eV for mc-Si lifetime samples, where the illumination condition was 2- to 10-fold higher than that used in this study (Liu et al., 2018a). Bredemeier et al. report an activation energy value of ~ 0.9 eV for the degradation process at a constant illumination intensity of 0.5 kW/m^2, with temperatures ranging from 75 to 120 °C (Bredemeier et al., 2017). This active energy is significantly higher than the value extracted in this work study. One possible reason is that recombination enhanced defect reactions that refers to any reaction path in which vibrational energy deposited locally at a defect by a nonradiative electronic transition serves to increase the reaction rate (L. C. Kimerling, 1978) reduce the activation energy when exposed to high injection levels.

The degradation rate (R_{deg}; Fig. 4(a)) and regeneration rate (R_{reg}; Fig. 4(b)) show a quadratic dependence on the excess carrier density (Δn) extracted from the corresponding relationship between solar intensity and excess carriers in the measured lifetime result list for as-fired samples, as well as the light intensity (not shown here). However, in the mc-Si, at processing temperature between 150 and 200 °C, the reaction rates for degradation have an approximate linear dependency on the applied illumination intensity (ranging from 14.6 kW/m^2 to 74.5 kW/m^2) (Liu et al., 2018a). A similar monotonicity of R_{deg} was observed with low Δn ($10^{13} \sim 10^{15}$) on mc-Si (Kwapil et al., 2017). The possible explanation for this inconsistence between the reported result for mc-Si and the present result for cast mono Si may be the uncertainty of R_{deg} and R_{reg}. As R_{deg} and R_{reg} depends on Δn, based on most likely a quadratic fit, and the excess carrier density changes with the lifetime throughout the course of degradation and regeneration reaction, a more complex relationship would be expected. Moreover, the measured degradation and regeneration rates were affected by each other, because regeneration likely proceeds in parallel with degradation (Bredemeier et al., 2017). However, as the regeneration kinetics are significantly

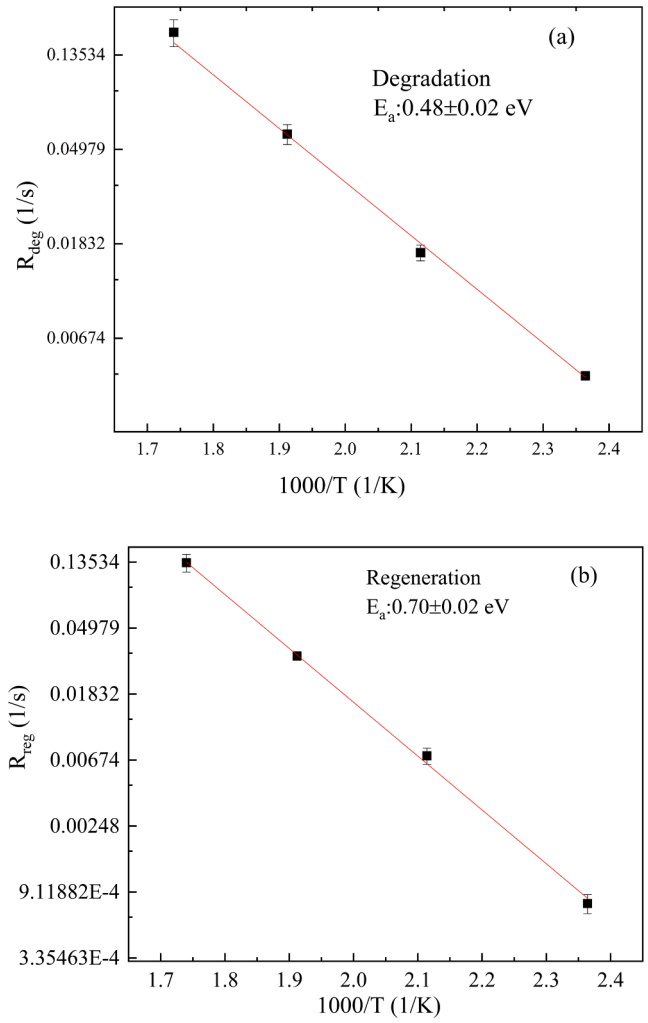

Fig. 3. Arrhenius correlations between the temperature and (a) degradation and (b) regeneration rate. The lines correspond to a linear fit to the Arrhenius analysis, yielding thermal activation energies of 0.48 and 0.70 eV for (a) and (b), respectively. The samples were light soaking at the temperature of 150 °C, 175 °C, 200 °C and 225 °C in the 7 suns.

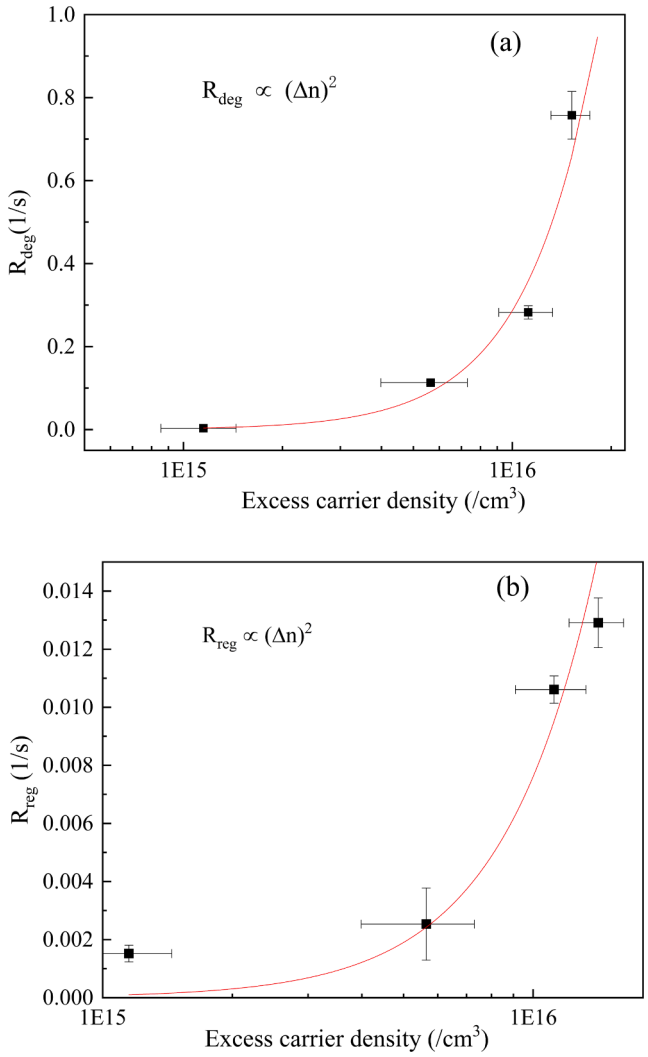

Fig. 4. (a) Degradation rate constants, R_{deg}, and (b) regeneration rate constants, R_{reg} for LS at 200 °C versus the excess carrier density Δn (filled squares) with a quadratic fit (solid line).

slower than the degradation kinetics, which is confirmed by the difference of defect Arrhenius activation energies between in the degradation and in regeneration stage, we assume that this impact is small, neglecting it in this study. The quadratic fits for R_{deg} and R_{reg} to Δn indicate that the supply of excess electrons determines the formation rate of the LeTID defects (Fig. 4). Moreover, an exponential of two suggests that the rate limiting step for each defect activation/formation involves two electrons. The initial compound, or at least one reaction material, therefore, involves a two-charge state.

The single-level defects has a nearly identical k_1 value at 28 ± 1 during the degradation process, which were extracted using the linear formulation based on SRH statistics, as shown in the samples from 2 to 80 s (Fig. 5 (a)). This value is similar to the k values in the range of 20 to 36 identified for the defect responsible for LeTID effects in other studies on mc-Si lifetime samples (Morishige et al., 2016; Chen et al., 2018). While non-linearity with X = n/p occurs when the LS time reaches up to 200. In these cases, the injection-dependence of the lifetime can be fitted with two single levels that act independently, i.e., $1/\tau_{SRH} = 1/\tau_1 + 1/\tau_2$, as shown Fig. 5(b). We can identify an additional k_2, which has only a weak impact on the lifetime and capture cross-section for electrons that is 0.4–1 units lower than that for holes at 300 K, i.e., mainly at a high injection (X greater than 0.5). Thus, the regeneration reaction introduces more than a simple single-level SRH recombination center. Along with the sample persistently regenerated until fully recovered, "Defect 2" became more dominant because it extended to the range of the low excess carrier density. The two defect states in the fully regenerated samples are with values of 53 ± 2 for k_1 and 0.4–1 for k_2. Especially for k_1, the larger uncertainty is due to error associated with the excess carrier density for the QSSPC measurement, which strongly affects the accuracy of measured lifetime data and induces k error in the range of ± 8. The error added to the tables is only related to the error for the fit and does not account for any other experimental uncertainties. However, the k_1 and k_2 values of regenerated samples are outside the range of k for the LeTID defect. This indicates that there is a contribution from another defect that increases the k, which may imply that the LeTID defect was gradually annealed or passivated by H during the regeneration process.

3.1.2. *Effect of dark annealing on LeTID*

Dark annealing of the regenerated state causes an effective increase in the lifetime. This increase occurs regardless of whether or not dark annealing has been performed before the first light soak. However, after dark annealing of the regenerated state, subsequent LS degrades the regenerated samples, with a smaller degradation extent than the previous LS, as shown in Fig. 6. This observation is similar to previous studies that their results show a reduction in the total degradation with each

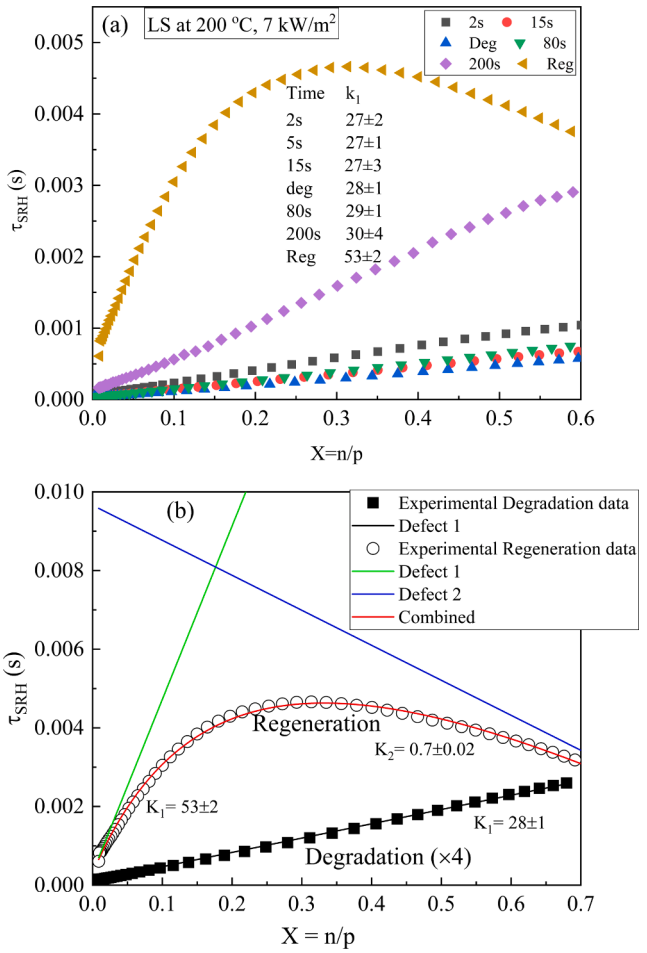

Fig. 5. (a) SRH lifetime of the LeTID defect for samples regenerated at 200 °C with a light intensity of 7 kW/m^2 as a function of X = n/p, Deg denotes degradation, Reg denotes regeneration. (b) The fit for the single and double defects for the SRH versus X curves for the degraded state (curve magnified 4-fold) and regenerated state (LS time: 400 s). The k_1 values extracted for the LS samples at different times are shown in (a).

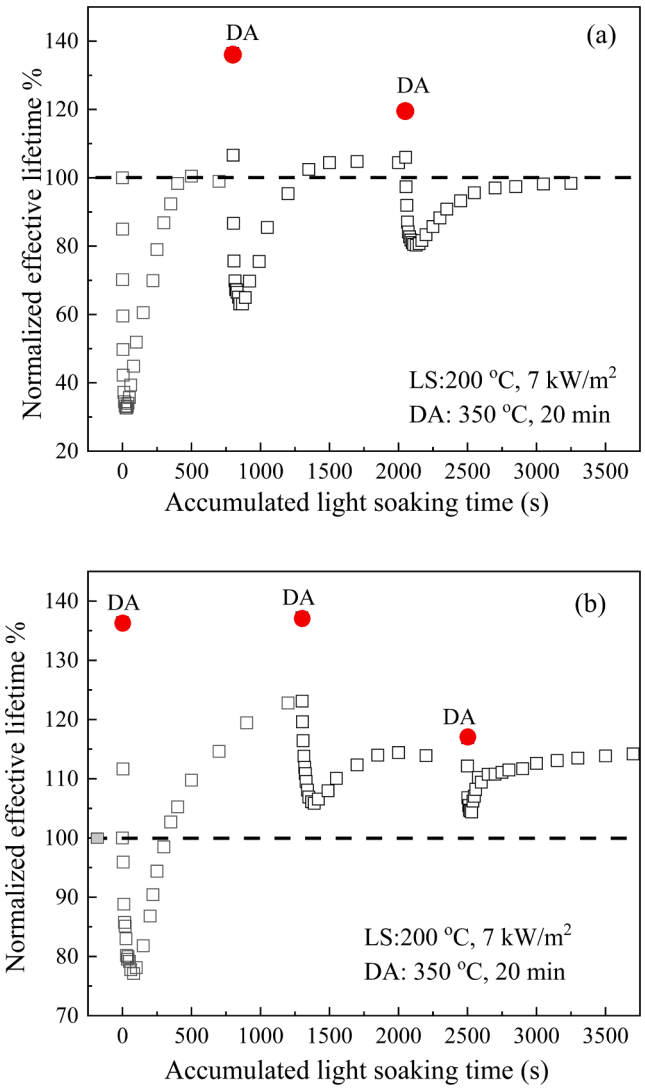

Fig. 6. Normalized effective minority lifetime (to the value directly after firing) extracted at a 1 × 10^{15} cm^{-3} injection level as a function of time when processed with an illumination of 7 kW/m^2 at 200 °C. The lifetime was monitored incrementally during illumination processing (black squares) and measured after a dark annealing process for 20 min at 350 °C (DA, red circle). (a) LS-DA cycle: fired sample first subjected to LS to the regenerated state, and then DA. This is the first LS-DA cycle, which is then repeated. (b) DA-LS cycle: fired samples first annealed in the dark, followed by LS until the lifetime attained a stable value. This is the first DA-LS cycle, which is then repeated twice. (For interpretation of the references to colour in this figure legend, the reader is referred to the web version of this article.)

DA-LS cycle (Chan et al., 2017). Moreover, in this study, the data show that dark annealing for the as-fired lifetime samples (before any LS) increases the final lifetime to a larger value than that of the as-fired samples (as shown in Fig. 6(b)). As suggested by Chen et al., a portion of the observed improvement to the lifetime during annealing in the dark is possibly associated with the annihilation of preexisting LeTID-related defects that formed during firing (Chen et al., 2018). The other improvements may have resulted from the H passivation of crystallographic defects and impurities, or other bulk defects. Moreover, dark annealing prior to light soaking (Fig. 6(b))) had a strong impact on the defect formation kinetics. The lifetime of the fired sample with annealing at 350 °C for 20 min prior to LS first increased by 35% due to solely the dark annealing process. Then, after LS, there was no more than 25% degradation relative to the lifetime of as-fired sample, which is significantly less degradation than the 70% observed during the first LS for the fired samples without DA (as shown in Fig. 6(a)). It is interesting to note that without DA before the LS, the lifetime in the regenerated state only recovers to the initial state (as-fired state) after each DA-LS cycle. But, for the as-fired sample with DA conducted before the first LS, even though the regenerated sample lifetimes are below the DA lifetimes, the stabilized lifetime for the regenerated samples after each DA-LS cycle is higher than the value for the as-fired samples.

Dark annealing had a strong impact on the defect reaction kinetics throughout both degradation and regeneration. As shown in Fig. 7, in the LS-DA cycle mode, the degradation and regeneration rates continuously decreased with an increase in the DA number. For example, the rate constants for degradation and regeneration decreased by 0.15 and 0.006 1/s, respectively, from the as-fired samples to the second DA cycle. In the DA-LS cycle mode, the degradation and regeneration rate constants remained nearly stable during the entire cycle while these values were also lower than the values for light illumination on the as-fired sample. Previous studies report that DA at a temperature lower than 225 °C accelerates the LeTID defect formation rate, whereas higher DA temperatures decelerated this formation rate on the mc-Si (Hang et al., 2018). A similar decrease in the degradation and regeneration rate after DA at higher temperatures was observed (Liu et al., 2018b). Earlier studies on mc-Si have concluded that the dark annealing process can actually alter the defect state, the availability of defect precursors, or otherwise alter the state of the defect system (Chan et al., 2017).

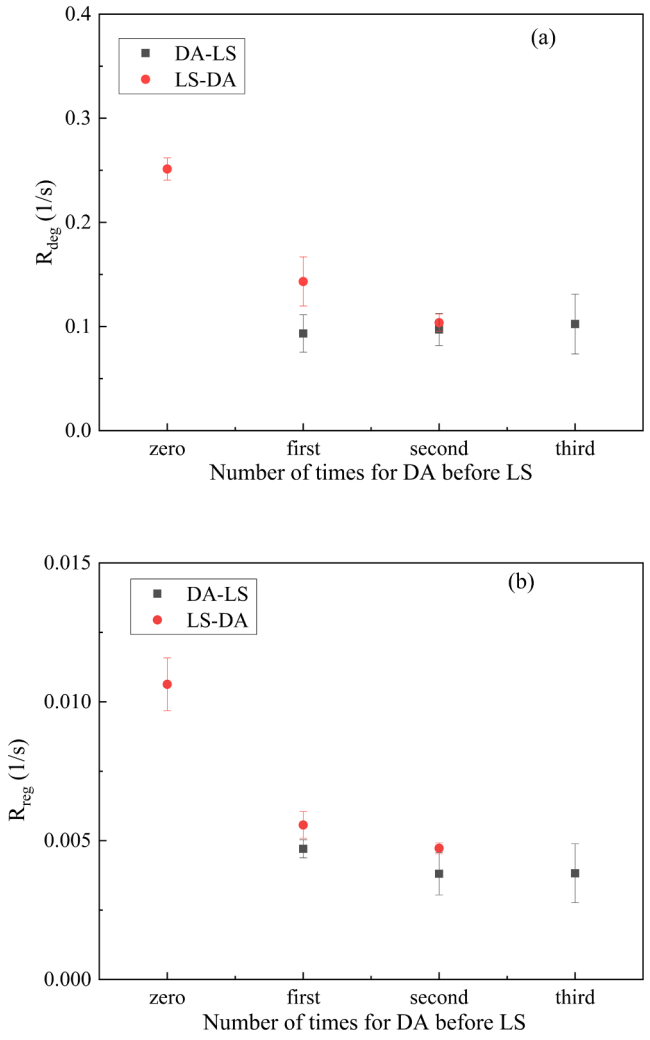

Fig. 7. Evolution of the degradation rate constant (a), and regeneration rate constant (b) for LeTID as a function of DA times before LS during LS-DA and DA-LS cycle experiment. DA: at 350 °C for 20 min; LS: at 200 °C with an illumination of 7 kW/m^2.

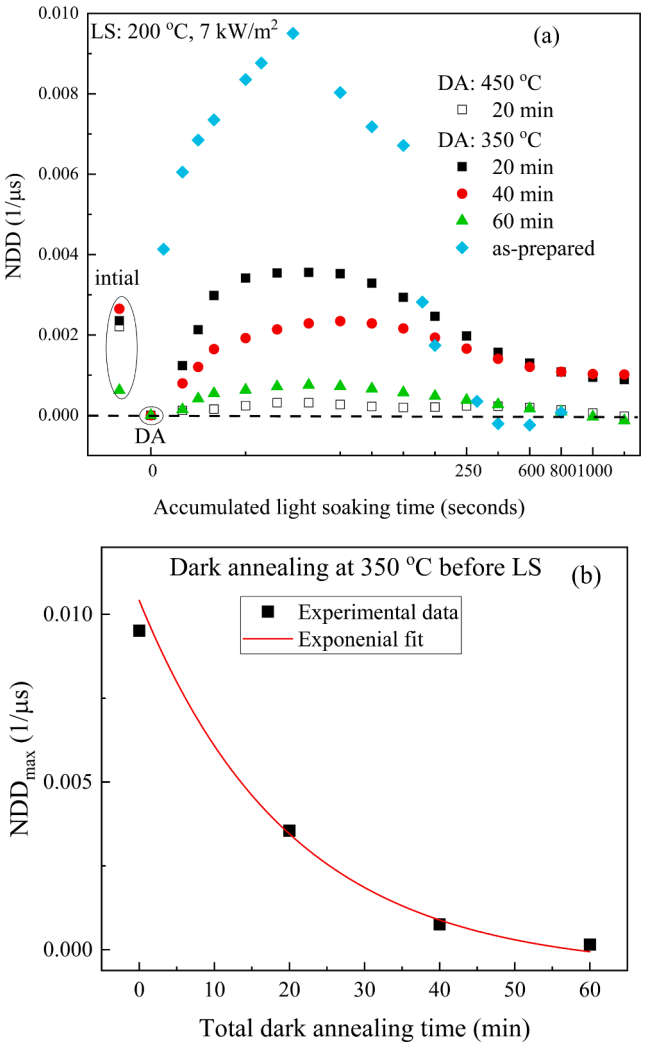

Fig. 8. Evolution of the NDD based on the effective minority carrier lifetime measurement at $\Delta n = 1 \times 10^{15}$ cm^{-3}. (a) NDD as a function of LS time under 7 sun illumination at 200 °C for samples annealed at 350 °C with different times from 20 to 60 min, as well as 450 °C for 20 min. The NDD for the as-fired and after annealing also is shown. (b) The maximum NDD extracted from (a) for samples under DA from 20 to 60 min at 350 °C before LS.

The maximum degradation value decreased with an increase in the annealing time and temperature. As shown in Fig. 8 (a), by increasing the accumulated annealing time, both the defect formation rates and recovery rates under LS slowed. For example, all samples reached the maximum degradation point between 40 and 60 s during light soaking at 200 °C and with a light intensity of 7 kW/m^2 compared to 400 s for as-fired samples. Fig. 8(b) shows a strong correlation occurs between the NDD_{max} and dark annealing time, which can be fitted using an exponential decay function. The results in this study are consistent with those reported in Fung et al., who discuss the LeTID effect on the mc-Si, where the maximum normalized defect density exponentially decreases with the number of cycles, suggesting that DA slowly depleted the defect precursors (Fung et al., 2018). They suggest that this change in the reaction rate is due to a change in the [B-H] as a result of DA. B-H should be the dominant source of LeTID defect precursors prior to light soaking (Hang et al., 2018). With different amounts of defect precursors present during light soaking, this eventually results in a modulation of the LeTID kinetics. Considering the similarity with the mentioned reported result above, the modulation of LeTID defects in cast mono silicon might be attributed to the B-H defect complex. In other words, annealing at 350 °C or higher temperature in the dark results in a decrease in the bulk B-H concentration compared to this concentration in the as-fired samples, such that a lower B-H concentration slows the reaction rate.

Although we observe similarities between the LeTID behavior of p-type cast mono Si and that of mc Si, including the defect formation and recovery energy, the ratio of the capture cross-section and the modulating kinetics may also be explained by the B-H concentration, but this requires another method combined with the lifetime test method to reveal the root cause.

3.2. *Stability test at 75 °C and 1 kW/m^2*

The LeTID stability test result in Fig. 9 shows DA for 20 min before LS regeneration has the most obvious effect on suppressing the degradation and improvements to the regeneration in the sample. This implies that this mixed process may be a potential method to provide both improved performance (the result in Fig. 6) and high anti-LeTID properties in Si PERC solar cells. As shown in Fig. 9a, if only DA is used, LeTID at 75 oC and 1 kW/m2 is not significantly suppressed (square data points). Furthermore, LS regeneration at 7 kW/m2 and temperature of 200 oC, which have been proven to provide the most stable cast mono Si PERC solar cells (Zhou et al., 2020), only provides a partial mitigation, with the degradation ratio to 12.5% and a shorter stability time of 100 h (circle data points). For samples with pre-annealing in the dark for 20

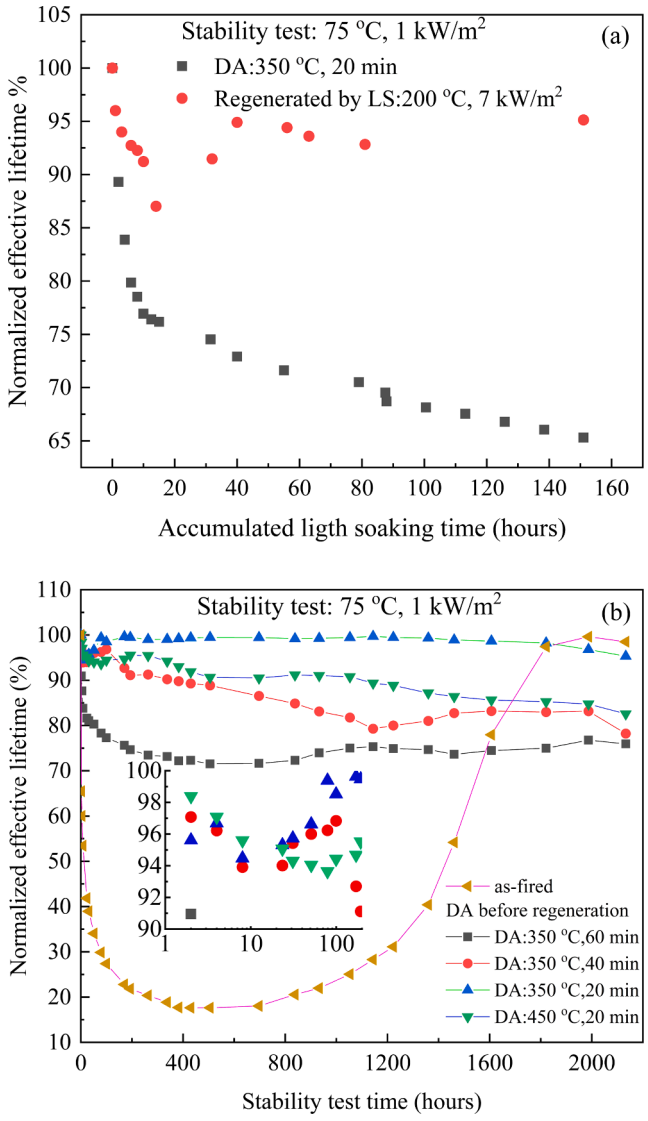

Fig. 9. Evolution of the lifetime during the stability test at 75 °C under 1 kW/m^2. (a) Samples regenerated at 200 °C under 7 kW/m^2 or annealing in the dark at 350 °C for 20 min. (b) Samples treated by DA at 350 °C for different times and then regenerated at 200 °C under 7 kW/m^2. As a reference, we present the as-prepared (as-fired) samples and samples treated by DA at 450 °C for 20 min and then regenerated at 200 °C under 7 kW/m^2 for 1200 s.

min at 350 °C, LS regeneration can further reduce the maximum degradation extent to ~ 5%, with the restoration of the minority carrier lifetime value to 100% within 100 h and stability up to 2000 h. Moreover, the degradation and regeneration rates are faster than those for the as-fired sample in which the effective lifetime decreases by 80% over 500 h, followed by a complete recovery over 2,000 h (Fig. 9(b)). Further increasing the DA time and temperature, there was a deceleration in the reaction rates for both the degradation and recovery during the LeTID stability test. Moreover, the degradation extent increases with an increase in the pre-annealing time and temperature during the stability test, which is contrary to the results for DA samples after the light soaking regeneration process (as shown in Fig. 8 (a)). We also note that until LeTID test for 2000 h, only the samples annealed at 350 °C before LS regeneration for 20 min and as-fired samples fully recovered to their initial lifetime, whereas the other samples became saturated at a recovered state of ~ 75–85% the initial lifetime. This long time degradation may mainly result from surface passivation degradation due to the long annealing time or high annealing temperature.

4. Conclusions

The kinetics of the degradation and subsequent regeneration in p-type cast mono wafers has been studied. The effect of light and substrate temperature on LeTID behavior is similar to the result of mc-Si and Cz-Si, but the thermal activation energies for LeTID-related degradation and regeneration were 0.48 ± 0.02 and 0.70 ± 0.02 eV, respectively, which were different from others. In addition, the effect of dark annealing on the LeTID behavior on p-type cast mono Si has been studied. Similar to the results for the mc-Si, kinetic modulation by the dark annealing may be affected by the B-H concentration while the effect of dark annealing can be explained by the defect reservoir theory. The dark annealing at 350 °C for 20 min before regeneration condition of 200 °C and illumination intensity of 7 kW/m^2 for 1200 s provides the most stable anti-LeTID performance and shortest recovery time within 100 h. The maximum degradation for the DA + LS treated lifetime samples was 5% compared with 12.5% for LS treated samples. In the absence of any light soaking or annealing (as-fired sample), the effective lifetime decreases by 80% over 500 h, followed by a complete recovery about 2,000 h. This implies that this DA + LS accelerated regeneration process may be a potential method to provide both improved performance and high anti-LeTID properties in Si PERC solar cells.

Declaration of Competing Interest

The authors declare that they have no known competing financial interests or personal relationships that could have appeared to influence the work reported in this paper.

Acknowledgments

This work has been supported by grants from the National Natural Science Foundation of China (Grant No.61874120), State Administration of Foreign Experts Affairs, China(Overseas Training project: P193041032), and by Norwegian Research Council (project 280909, 261574). The authors would like to thank the processing team in the Solar Energy Department (IFE, Norway) for assistance with processing in this work, in particular, Marie Syre Wiig, and Halvard Haug.

References

Bredemeier, D., et al., 2017. Light-induced lifetime degradation in high-performance multicrystalline silicon: Detailed kinetics of the defect activation. Sol. Energy Mater. Sol. Cells 173, 2–5.
Chan, C., et al., 2017. Modulation of carrier-induced defect kinetics in multi-crystalline silicon PERC cells through dark annealing. Sol. RRL 1, 1600028.
Chen, D., et al., 2017. Evidence of an identical firing-activated carrier-induced defect in monocrystalline and multicrystalline silicon. Sol. Energy Mater. Sol. Cells 172, 293–300.
Chen, D., et al., 2018. Hydrogen induced degradation: A possible mechanism for light- and elevated temperature- induced degradation in n-type silicon. Sol. Energy Mater. Sol. Cells 185, 174–182.
Eberle, R., et al., 2016. Impact of the firing temperature profile on light induced degradation of multicrystalline silicon. Physica Status Solidi Rapid Research Letters 10, 861–865.
Fung, T.H., et al., 2018. A four-state kinetic model for the carrier-induced degradation in multicrystalline silicon: Introducing the reservoir state. Sol. Energy Mater. Sol. Cells 184, 48–56.
Hang, F.T., et al., 2018. Influence of bound hydrogen states on carrier-induced degradation in multi-crystalline silicon. AIP Conf. Proc. 1999, 130004.
Kaden, T., et al., 2012. Analysis of mono- cast silicon wafers and solar cells on industrial scale. Energy Procedia 27, 103–108.
Kimerling, L.C., 1978. Recombination enhanced defect reactions. Solid-State Electronic 21, 1391–1401.
Kwapil, W., Niewelt, T., Schubert, M.C., 2017. Kinetics of carrier-induced degradation at elevated temperature in multicrystalline silicon solar cells. Sol. Energy Mater. Sol. Cells 173, 80–84.
Kutsukake, K., et al., 2014. Mono-Like Silicon Growth Using Functional Grain Boundaries to Limit Area of Multicrystalline Grains. IEEE Journal of Photovoltaics 4, 84–87.
Liu, S.Y., et al., 2018a. Investigation of temperature and illumination dependencies of carrier-induced degradation in p-type multi-crystalline silicon, SiliconPV, The 8th international Conference on Crystalline Silicon Photovoltics, 130014.

Liu, S.Y., et al., 2018. Impact of Dark Annealing on the Kinetics of Light-and Elevated-Temperature-Induced Degradation. IEEE Journal of Photovoltaics 8, 1494–1502.
Luka, T., et al., 2016. Intra-grain versus grain boundary degradation due to illumination and annealing behavior of multi-crystalline solar cells. Sol. Energy Mater. Sol. Cells 158, 43–49.
Lv, Y., et al., 2020. Towards high-efficiency industrial p-type mono-like Si PERC solar cells. Sol. Energy Mater. Sol. Cells 204, 110202.
Morishige, A.E., et al., 2016. Lifetime Spectroscopy Investigation of Light-Induced Degradation in p-type Multicrystalline Silicon PERC. IEEE Journal of Photovoltaics 6, 1466–1472.
Murphy, J.D., et al., 2012. Parameterisation of injection-dependent lifetime measurements in semiconductors in terms of Shockley-Read-Hall statistics: An application to oxide precipitates in silicon. J. Appl. Phys. 111, 113709.
Nagel, H., Berge, C., Aberle, A., 1999. Generalized analysis of quasi-steady-state and quasi-transient measurements of carrier lifetimes in semiconductors. J. Appl. Phys. 86, 6218–6221.
Niewelt, T., et al., 2017a. Light-induced activation and deactivation of bulk defects in boron-doped float-zone silicon. J. Appl. Phys. 121, 185702.
Niewelt, T., et al., 2017b. Degradation of Crystalline Silicon Due to Boron-Oxygen Defects. IEEE Journal of Photovoltaics 7, 383–398.
Nickel, N.H., Anderson, G.B., Walker, J., 1996. Hydrogen-induced platelets in disordered silicon. Solid State Communications 99, 427–431.
Ramspeck, K., et al., 2012. Light induced degradation of rear passivated mc-Si solar cells, in: Proc. 27th Eur. Photovoltaic Solar Energy Conf., pp. 861-865.
Sio, H.C., et al., 2018. Light and elevated temperature induced degradation in p-type and n-type cast-grown multicrystalline and mono-like silicon. Sol. Energy Mater. Sol. Cells 182, 98–104.
Stoddard, N., et al., 2016. On the potential and limits of large area seeding for photovoltaic silicon. J. Cryst. Growth 452, 272–275.
Takahashi, I., et al., 2015. Seed manipulation for artificially controlled defect technique in new growth method for quasi-monocrystalline Si ingot based on casting. Appl. Phys. Express. 8, 105501.
Vahlman, H., et al., 2017. Light-induced degradation in quasi-monocrystalline silicon PERC solar cells: Indications on involvement of copper. Physica Status Solidi (a). 214, 1700321.
Vargas, C., et al., 2019. Degradation and recovery of n-type multi-crystalline silicon under illuminated and dark annealing conditions at moderate temperatures. IEEE Journal of Photovoltaics 9, 355–363.
Ye, F., et al., 2018. UV-induced degradation in multicrystalline PERC cell and module. Solar Energy 170, 1009–1015.
Zhou, C.L., et al., 2020. Light and elevated temperature induced degradation in B-Ga co-doped cast mono Si PERC solar cells. Sol. Energy Mater. Sol. Cells 211, 110508.
Zuschlag, A., Skorka, D., Hahn, G., 2017. Degradation and regeneration in mc-Si after different gettering steps. Prog. Photovoltaics: Research and Applications 25, 545–552.